SU(3)-flavor breaking in octet baryon masses and axial couplings

Manuel E. Carrillo-Serrano,[1] Ian C. Cloët,[2] and Anthony W. Thomas[1]
[1]*CSSM and ARC Centre of Excellence for Particle Physics at the Tera-scale, School of Chemistry and Physics, University of Adelaide, Adelaide SA 5005, Australia*
[2]*Physics Division, Argonne National Laboratory, Argonne, Illinois 60439, USA*
(Received 15 September 2014; revised manuscript received 6 December 2014; published 23 December 2014)

The lightest baryon octet is studied within a covariant and confining Nambu–Jona-Lasinio model. By solving the Poincaré covariant Faddeev equations—including scalar and axialvector diquarks—we determine the baryon octet masses and axial charges for strangeness conserving transitions. For the axial charges the degree of violation of SU(3) flavor symmetry, arising because of the strange spectator quark(s), is found to be no more than 10%.

DOI: 10.1103/PhysRevC.90.064316 PACS number(s): 12.39.Ba, 12.39.Fe, 13.30.Ce, 14.20.Jn

I. INTRODUCTION

In the quest to fully understand quantum chromodynamics (QCD) it is not sufficient to study baryons whose valence quark content consists only of the light u and d quarks. A solid understanding of all members of the baryon octet—that is, the nucleon, Λ, Σ, and Ξ multiplets—remains a critical step. Early work on their structure centered on the constituent quark model [1,2] and the MIT bag model [3], later supplemented by chiral corrections associated with the cloud of virtual pions and kaons that are important components of a baryon wave function [4–12]. Once their basic properties, such as masses, charge radii, magnetic moments, and axial charges had been calculated, attention naturally turned to more complex properties, such as their parton distribution functions [13,14].

The empirical evidence concerning the structure of the hyperons is naturally far more limited than for nucleons. While there exists fairly good data for octet baryon masses, magnetic moments, and axial charges [15], little or nothing is known about, e.g., their electromagnetic or axial form factors as a function of momentum transfer. Finding ways to explore these properties experimentally would be very valuable. On the other hand, over the last couple of decades lattice QCD has made steady progress in the calculation of octet baryon masses [16–19], including determinations of their isospin mass splittings [20] and certain electroweak matrix elements [21]. These studies have been complemented by a judicious use of chiral effective field theory to extrapolate to the physical quark masses. Thus, we now have quite accurate determinations of the hyperon electric [22] and magnetic [23] form factors up to $1.4\,\mathrm{GeV}^2$, as well as low moments of their parton distribution functions [24]. It has even been possible recently to shed some light on the proton spin puzzle [25,26] by calculating the spin fractions carried by quarks across the octet [27].

On general grounds one would prefer to have models of octet baryon properties that are covariant and respect the symmetries of QCD. The former is especially important if one wants to investigate parton distribution functions and form factors, at even moderate momentum transfer. The hope in building more sophisticated models is that through comparison with empirical data and lattice QCD studies, one may develop a deeper understanding of how QCD works in the nonperturbative regime. For example, exploring issues such as the importance and role of diquark correlations and chiral corrections [28], as well as the transition from nonperturbative to perturbative QCD [29].

In this work we investigate the masses and strangeness conserving ($\Delta S = 0$) axial charges of the octet baryons within the framework of the covariant model of Nambu and Jona-Lasinio (NJL) [30–34], where confinement is simulated by employing proper-time regularization [35–37]. Octet baryons are described by a Poincaré covariant Faddeev equation, where scalar and axialvector diquark correlations play a critical role. Flavor breaking effects, introduced by a dressed strange quark that turns out to be approximately 50% heavier that the dressed light quarks, will also be studied.

The structure of the paper is as follows: Sec. II provides a brief introduction to the NJL model, including a discussion of the Bethe-Salpeter equation for mesons and diquarks. Section III introduces the Faddeev equation for octet baryons, discussing the solution for the Poincaré covariant Faddeev amplitude and octet masses. Finally, in Sec. V, the formalism is used to determine the axial charges associated with strangeness conserving beta decays. Section VI summarizes our findings and presents some concluding remarks.

II. NAMBU–JONA-LASINIO MODEL

The NJL model was formulated as a theory of elementary fermions which encapsulated dynamical chiral symmetry breaking in a transparent manner [30,31]. With the advent of QCD, the NJL model was reformulated with quarks as the fundamental degrees of freedom, such that the symmetries of QCD are respected.[1] In particular the NJL model exhibits dynamical chiral symmetry breaking, which, as implemented in this work, gives rise to approximately 95% of the nucleon mass.

The complete three-flavor NJL Lagrangian in the $\bar{q}q$ interaction channel—including only 4-fermion interactions—has the form [34],

$$\mathcal{L} = \bar{\psi}(i\,\partial\!\!\!/ - \hat{m})\psi + \tfrac{1}{2}\,G_\pi\big[\tfrac{2}{3}(\bar{\psi}\,\psi)^2 + (\bar{\psi}\,\boldsymbol{\lambda}\,\psi)^2 - \tfrac{2}{3}(\bar{\psi}\,\gamma_5\,\psi)^2 - (\bar{\psi}\,\gamma_5\,\boldsymbol{\lambda}\,\psi)^2\big]$$

[1]The SU(3) color gauge symmetry of QCD is a global symmetry of the NJL model.

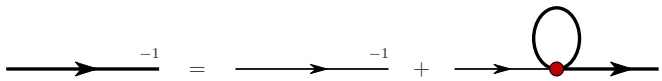

FIG. 1. (Color online) The NJL gap equation in the Hartree-Fock approximation, where the thin line represents the elementary quark propagator, $S_{0q}^{-1}(k) = \not{k} - m_q + i\varepsilon$, and the shaded circle represents the 4-fermion interaction.

$$-\tfrac{1}{2}\,G_\rho[(\bar\psi\,\gamma^\mu\,\boldsymbol{\lambda}\,\psi)^2 + (\bar\psi\,\gamma^\mu\gamma_5\,\boldsymbol{\lambda}\,\psi)^2] - \tfrac{1}{2}\,G_0(\bar\psi\,\gamma^\mu\,\psi)^2 - \tfrac{1}{2}\,G_5(\bar\psi\,\gamma^\mu\gamma_5\,\psi)^2, \quad (1)$$

where $\boldsymbol{\lambda}$ represents the eight Gell-Mann matrices and $\hat m = \mathrm{diag}\,[m_u, m_d, m_s]$. The NJL model does not include gluons as explicit degrees of freedom, as such the pointlike quark-quark interaction renders the NJL model nonrenormalizable. We regularize the NJL model using the proper-time scheme, which maintains Lorentz and gauge invariance; it also removes unphysical thresholds for the decay of color singlet bound states into their colored constituents, thereby simulating quark confinement [35–37].

The dressed quark propagator in the NJL model is obtained from the gap equation illustrated in Fig. 1. The solution for a quark of flavor $q = u, d, s$ has the form,

$$S_q^{-1}(k) = \not{k} - M_q + i\varepsilon, \quad (2)$$

where, in the proper-time regularization scheme, the dressed quark masses each satisfy

$$M_q = m_q + \frac{3}{\pi^2}\,M_q\,G_\pi \int_{1/\Lambda_{UV}^2}^{1/\Lambda_{IR}^2} d\tau\,\frac{e^{-\tau M_q^2}}{\tau^2}. \quad (3)$$

In this three-flavor NJL model, defined by Eq. (1), the gap equation does not introduce flavor mixing in the quark propagator; this is in contrast to the two-flavor case which in general has flavor mixing [34].

The quark-quark interaction needed for the two-body interaction kernel in the Faddeev equation (to be described shortly) can be obtained from Eq. (1) using Fierz transformations. Keeping only scalar and axialvector diquark correlations, the NJL interaction Lagrangian in the qq channel reads

$$\mathcal{L}_I^{qq} = G_s[\bar\psi\,\gamma_5\,C\,\lambda_a\,\beta_A\,\bar\psi^T][\psi^T\,C^{-1}\gamma_5\,\lambda_a\,\beta_A\,\psi] + G_a[\bar\psi\,\gamma_\mu\,C\,\lambda_s\,\beta_A\,\bar\psi^T][\psi^T\,C^{-1}\gamma^\mu\,\lambda_s\,\beta_A\,\psi], \quad (4)$$

where $C = i\gamma_2\gamma_0$ is the charge conjugation matrix and the couplings G_s and G_a give the strength of the scalar and axialvector qq interactions.[2] The flavor matrices are labeled by $\lambda_a = \lambda_2, \lambda_5, \lambda_7$ and $\lambda_s = \lambda_0, \lambda_1, \lambda_3, \lambda_4, \lambda_6, \lambda_8$, where $\lambda_0 \equiv \sqrt{\frac{2}{3}}\,\mathbb{1}$. Thus, there are three types of scalar and six types of axialvector diquarks. The color $\bar 3$ matrices are given by $\beta_A = \sqrt{\frac{3}{2}}\,\lambda_A (A = 2,5,7)$ [38–40] and hence the interaction terms in Eq. (4) are totally antisymmetric, as demanded by the Pauli principle.

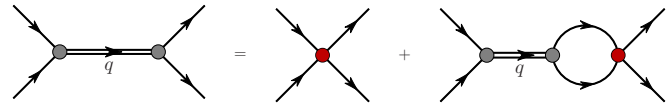

FIG. 2. (Color online) Inhomogeneous Bethe-Salpeter equation for quark-quark (diquark) correlations.

Quark-antiquark and quark-quark bound states are obtained by solving the appropriate Bethe-Salpeter equation, which is illustrated in Fig. 2 for diquarks. The reduced t matrices for scalar and axialvector diquarks, with quark flavor content q_1 and q_2, take the form,[3]

$$\tau_{[q_1q_2]}(q) = \frac{-4i\,G_s}{1 + 2\,G_s\,\Pi_{[q_1q_2]}(q^2)}, \quad (5)$$

$$\tau^{\mu\nu}_{\{q_1q_2\}}(q) = \frac{-4i\,G_a}{1 + 2\,G_a\,\Pi_{\{q_1q_2\}}(q^2)} \times \left[g^{\mu\nu} + 2\,G_a\,\Pi_{\{q_1q_2\}}(q^2)\,\frac{q^\mu q^\nu}{q^2}\right]. \quad (6)$$

The bubble diagrams are given by

$$\Pi_{[q_1q_2]}(q^2) = 6i\int\frac{d^4k}{(2\pi)^4}\,\mathrm{Tr}[\gamma_5\,S_{q_1}(k)\,\gamma_5\,S_{q_2}(k+q)], \quad (7)$$

$$\Pi_{\{q_1q_2\}}(q^2)\left(g^{\mu\nu} - \frac{q^\mu q^\nu}{q^2}\right) = 6i\int\frac{d^4k}{(2\pi)^4}\,\mathrm{Tr}\left[\gamma^\mu\,S_{q_1}(k)\,\gamma^\nu\,S_{q_2}(k+q)\right], \quad (8)$$

where the flavor and color traces have been taken, and the remaining trace is over Dirac indices only. The masses of the various diquarks are given by the poles in the corresponding t matrix, e.g., the scalar diquarks masses are given by the pole condition,

$$1 + 2\,G_s\,\Pi_{[q_1q_2]}\left(q^2 = M^2_{[q_1q_2]}\right) = 0. \quad (9)$$

For the octet baryon calculations we approximate the full diquark t matrix by a *contact* + *pole* form [37], that is,

$$\tau_{[q_1q_2]}(q) \to 4i\,G_s - \frac{i\,Z_{[q_1q_2]}}{q^2 - M^2_{[q_1q_2]} + i\,\varepsilon}, \quad (10)$$

$$\tau^{\mu\nu}_{\{q_1q_2\}}(q) \to 4i\,G_a - \frac{i\,Z_{\{q_1q_2\}}}{q^2 - M^2_{\{q_1q_2\}} + i\,\varepsilon}\left(g^{\mu\nu} - \frac{q^\mu q^\nu}{M^2_{\{q_1q_2\}}}\right), \quad (11)$$

[2] In principle the coupling in the $\bar qq$ Lagrangian of Eq. (1) are formally related to the coupling appearing in the qq Lagrangian of Eq. (4), as detailed in Appendix A of Ref. [38]. However, to increase the flexibility of our model, these form relations are not retained and each coupling is separately fit to data, as explained in Sec. IV.

[3] Throughout this paper $[q_1q_2]$ will indicate a quantity associated with a scalar diquark and $\{q_1q_2\}$ will indicate a quantity associated with an axialvector diquark.

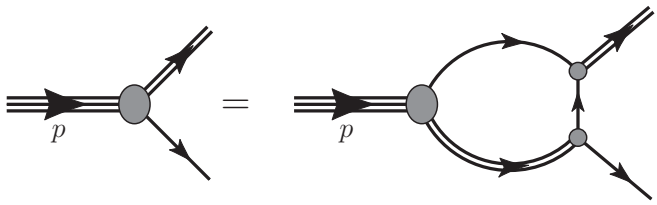

FIG. 3. Homogeneous Poincaré covariant Faddeev equation whose solution gives the mass and vertex function for each member of the baryon octet.

where the pole residues are given by

$$Z^{-1}_{[q_1q_2]} = -\frac{1}{2}\frac{\partial}{\partial q^2}\,\Pi_{[q_1q_2]}(q^2)\Big|_{q^2=M^2_{[q_1q_2]}}, \tag{12}$$

$$Z^{-1}_{\{q_1q_2\}} = -\frac{1}{2}\frac{\partial}{\partial q^2}\,\Pi_{\{q_1q_2\}}(q^2)\Big|_{q^2=M^2_{\{q_1q_2\}}}. \tag{13}$$

III. FADDEEV EQUATIONS FOR OCTET BARYONS

Octet baryons are constructed as solutions to a Poincaré covariant Faddeev equation, which is illustrated in Fig. 3, where the quark-diquark approximation used here was made explicit [41]. A tractable solution to the Faddeev equation is obtained by employing the static approximation [42] to the quark exchange kernel, where the exchanged quark propagator becomes $S_q(k) \to -\frac{1}{M_q}$. This approximation was shown to yield excellent results for nucleon form factors [28] and quark distributions [43–46]. The Faddeev equation for each octet baryon then takes the form,

$$\Gamma_B(p,s) = Z_B\,\Pi_B(p)\,\Gamma_B(p,s), \tag{14}$$

where B labels an octet baryon, Z_B the corresponding quark exchange kernel, and $\Pi_B(p)$ is a diagonal matrix containing the various combinations of quark and diquark propagator. Equation (14) must be supplemented by a normalization condition, such that the normalized Faddeev vertex reads

$$\Gamma_B(p,s) = \sqrt{-\mathcal{Z}_B}\;\Gamma_{0B}(p,s), \tag{15}$$

where $\Gamma_{0B}(p,s)$ is the unnormalized vertex and the normalization condition that determines $\mathcal{Z}_B$ will be discussed shortly.

For equal light quark masses the nucleon, Σ, and Ξ Faddeev vertex functions contain one scalar and two types of axialvector diquarks,[4] with a Dirac structure of the form,

$$\Gamma_b(p,s) = \begin{bmatrix} \Gamma_{q_1[q_1q_2]}(p,s) \\ \Gamma^\mu_{q_1\{q_1q_2\}}(p,s) \\ \Gamma^\mu_{q_2\{q_1q_1\}}(p,s) \end{bmatrix}, \tag{16}$$

$$= \sqrt{-\mathcal{Z}_b}\begin{bmatrix} \alpha_1 \\ \alpha_2\,\frac{p^\mu}{M_b}\,\gamma_5 + \alpha_3\,\gamma^\mu\gamma_5 \\ \alpha_4\,\frac{p^\mu}{M_b}\,\gamma_5 + \alpha_5\,\gamma^\mu\gamma_5 \end{bmatrix} u_b(p,s), \tag{17}$$

where $b = [\text{nucleon}, \Sigma, \Xi]$ and $\mathcal{Z}_b$ is the vertex normalization. The Faddeev vertex function for the Λ baryon, with equal u and d quark masses, contains two types of scalar diquarks and an axialvector diquark and therefore reads

$$\Gamma_\Lambda(p,s) = \sqrt{-\mathcal{Z}_\Lambda}\begin{bmatrix} \alpha_1 \\ \alpha_2 \\ \alpha_3\,\frac{p^\mu}{M_\Lambda}\,\gamma_5 + \alpha_4\,\gamma^\mu\gamma_5 \end{bmatrix} u_\Lambda(p,s). \tag{18}$$

The quark exchange kernel for the nucleon, Σ, and Ξ reads

$$Z_b = 3\begin{bmatrix} \frac{1}{M_1} & \frac{1}{M_1}\gamma_\sigma\gamma_5 & -\frac{\sqrt{2}}{M_2}\gamma_\sigma\gamma_5 \\ \frac{1}{M_1}\gamma_5\gamma_\mu & \frac{1}{M_1}\gamma_\sigma\gamma_\mu & \frac{\sqrt{2}}{M_2}\gamma_\sigma\gamma_\mu \\ -\frac{\sqrt{2}}{M_2}\gamma_5\gamma_\mu & \frac{\sqrt{2}}{M_2}\gamma_\sigma\gamma_\mu & 0 \end{bmatrix}, \tag{19}$$

where, in each case, M_1 is the mass of the singly represented dressed quark and M_2 the mass of the doubly represented dressed quark.[5] The factor of 3 is obtained from projecting the kernel onto color singlet states. For the Λ the quark exchange kernel is given by

$$Z_\Lambda = \begin{bmatrix} 0 & \frac{\sqrt{2}}{M_\ell} & -\frac{\sqrt{2}}{M_\ell} \\ \frac{\sqrt{2}}{M_\ell} & -\frac{1}{M_s} & -\frac{1}{M_s}\gamma_\sigma\gamma_5 \\ -\frac{\sqrt{2}}{M_\ell}\gamma_5\gamma_\mu & -\frac{1}{M_s}\gamma_5\gamma_\mu & -\frac{1}{M_s}\gamma_\sigma\gamma_\mu \end{bmatrix}, \tag{20}$$

where M_ℓ is the mass of the dressed light quark. The quark-diquark bubble diagram matrix for the nucleon, Σ, and Ξ reads

$$\Pi_b(p) = \begin{bmatrix} \Pi_{q_2[q_1q_2]}(p) & 0 & 0 \\ 0 & \Pi^{\sigma\nu}_{q_2\{q_1q_2\}}(p) & 0 \\ 0 & 0 & \Pi^{\sigma\nu}_{q_1\{q_2q_2\}}(p) \end{bmatrix}, \tag{21}$$

where for each baryon q_1 is the singly represented dressed quark and q_2 the doubly represented dressed quark. For the Λ the analogous quantity reads

$$\Pi_\Lambda(p) = \begin{bmatrix} \Pi_{s[\ell\ell]}(p) & 0 & 0 \\ 0 & \Pi_{\ell[\ell s]}(p) & 0 \\ 0 & 0 & \Pi^{\sigma\nu}_{\ell\{\ell s\}}(p) \end{bmatrix}. \tag{22}$$

The quark-diquark bubble diagrams are given by

$$\Pi_{q_i[q_jq_k]}(p) = \int \frac{d^4k}{(2\pi)^4}\,S_{q_i}(k)\,\tau_{[q_jq_k]}(p-k), \tag{23}$$

$$\Pi^{\mu\nu}_{q_i\{q_jq_k\}}(p) = \int \frac{d^4k}{(2\pi)^4}\,S_{q_i}(k)\,\tau^{\mu\nu}_{\{q_jq_k\}}(p-k). \tag{24}$$

[4] For the nucleon, in the $M_u = M_d$ limit, the singly and doubly represented axialvector diquarks are mass degenerate and could therefore be treated as a single type of diquark. However, for the nucleon we will keep the description more general so that the analogy with the other members of the octet is straightforward.

[5] For the Σ^0, the term "doubly represented" means the two light quarks of different flavors.

TABLE I. Model parameters are constrained to reproduce the physical pion and ρ meson masses, the pion decay constant, the nucleon and Ξ masses, and the nucleon axial coupling. The infrared regulator and the dressed u and d quark masses—labeled by M_ℓ—are assigned their values *a priori*. The regularization parameters and dressed quark mass are in units of GeV, while the couplings are in units of GeV $^{-2}$.

$\Lambda_{\rm IR}$	$\Lambda_{\rm UV}$	M_ℓ	M_s	G_π	G_ρ	G_s	G_a
0.240	0.645	0.40	0.59	19.0	10.8	7.6	2.6

Finally, the vertex normalization is given by

$$\mathcal{Z}_B^{-1} = \overline{\Gamma}_{0B}\, \frac{\partial \Pi_B(p)}{\partial p^2}\, \Gamma_{0B}\Big|_{p^2=M_B^2}. \tag{25}$$

Note, the value of p^2 which satisfies the Faddeev equation for each octet baryon defines its mass M_B^2, and at that point the coefficients α_i then define the octet baryon vertex function.

IV. RESULTS FOR OCTET BARYONS MASSES

The NJL model employed in this work has the following parameters: two regularization parameters $\Lambda_{\rm IR}$ and $\Lambda_{\rm UV}$; the dressed quark masses M_u, M_d, and M_s;[6] two coupling constants, G_π and G_ρ, from the $\bar{q}q$ NJL Lagrangian, given in Eq. (1); and the two coupling constants G_s and G_a from the qq NJL Lagrangian. The infrared cutoff implements confinement and therefore should be of the order of $\Lambda_{\rm QCD}$ and we choose $\Lambda_{\rm IR} = 0.240\,$GeV; for the light-quark dressed masses we take $M_u = M_d = 0.4\,$GeV; the ultraviolet cutoff $\Lambda_{\rm UV}$ and the couplings G_π and G_ρ are constrained by the empirical values for the pion decay constant, the pion mass and the ρ mass; the qq couplings are chosen to reproduce the physical nucleon mass and the nucleon axial coupling constant. Finally, the dressed s-quark mass is fixed to reproduce the empirical mass of the cascade baryon (Ξ). The resulting parameters are summarized in Table I.

Results for the kaon mass together with the various diquark masses are given in Table II. The splitting between the various scalar diquarks and between the axialvector diquarks is the result of explicit SU(3)$_F$ breaking effects from the strange quark. The empirical light to strange current quark mass ratio in the $\overline{\rm MS}$ regularization scheme is $m_s/m_q = 27.5 \pm 1.0$ [15], while we find $m_s/m_q = 21.7$. For the analogous dressed quark mass ratio we obtain $M_s/M_q \simeq 1.5$, which illustrates that effects from DCSB are very much suppressed for the heavier strange quark. For completeness we give in Table III the pole residues for the meson and diquark t matrices.

[6]Alternatively, one may use the current quark masses m_u, m_d, m_s from the NJL Lagrangian, as the gap equation provides a one-to-one correspondence with the dressed masses.

TABLE II. Results for the kaon mass, together with the various diquark masses, where the subscript $\ell = u, d$. Recall that the square brackets label scalar diquarks and the curly brackets axialvector diquarks. All masses are in units of GeV.

M_K	$M_{[\ell\ell]}$	$M_{[\ell s]}$	$M_{\{\ell\ell\}}$	$M_{\{\ell s\}}$	$M_{\{ss\}}$
0.47	0.68	0.85	1.04	1.17	1.30

TABLE III. Results for the pole residues in the various meson and diquark t matrices [c.f. Eqs. (10) and (11)].

Z_π	Z_K	$Z_{[\ell\ell]}$	$Z_{[\ell s]}$	$Z_{\{\ell\ell\}}$	$Z_{\{\ell s\}}$	$Z_{\{ss\}}$
17.8	29.6	14.8	16.4	3.56	3.93	4.29

The octet baryon masses obtained by solving the appropriate Faddeev equation, as discussed in Sec. III, are given in Table IV. In the SU(3)-flavor limit all octet baryon masses are degenerate and hence the mass splitting between octet baryons results solely from the heavier s-quark mass. The mass splitting between the Λ and Σ baryons is a consequence of the different diquark correlations which dominate their wave functions. The Λ baryon contains two types of scalar diquarks and one type of axialvector diquark—$[\ell\ell]$, $[\ell s]$, and $\{\ell s\}$—while the Σ baryon contains one type of scalar diquark and two types of axialvector diquarks—$[\ell s]$, $\{\ell s\}$, and $\{\ell\ell\}$. Scalar diquarks are more bound than axialvector diquarks—because of their strong connection with the pion and DCSB—and consequently we find that the Λ is approximately 110 MeV lighter than the Σ baryon. This is in reasonable agreement with the empirical mass splitting of approximately 80 MeV. A more precise fit would also need to include chiral corrections. The parameters defining the Faddeev vertex function for each member of the baryon octet are summarized in Table V.

V. AXIAL CHARGES

The axial charges of the baryons are important because they connect the strong and weak interactions. They are also related to the quark spin content of the baryons [47]. In fact, assuming SU(3)-flavor symmetry, all octet baryon decays can be parametrized by just three quantities: the Cabbibo angle, θ_C, and the F and D couplings [48,49].

The axial current of an octet baryon has the form,

$$\begin{aligned} J^{\mu,a}_{5,\lambda'\lambda}(p',p) &= \langle p',\lambda'|\bar{\psi}_q\,\gamma^\mu\gamma_5\,\lambda_a\,\psi_q|p,\lambda\rangle, \\ &= \bar{u}(p',\lambda')\Big[\gamma^\mu\gamma_5\,G_A(Q^2) + \frac{q^\mu\gamma_5}{2\,M_B}\,G_P(Q^2) \\ &\quad + \frac{i\sigma^{\mu\nu}q_\nu\,\gamma_5}{2\,M_B}\,G_T(Q^2)\Big]\lambda_a\,u(p,\lambda), \end{aligned} \tag{26}$$

TABLE IV. Results for octet baryon masses and the average experimental mass for the corresponding multiplet. All experimental masses have an error of at most 0.015% but usually it is much less [15]. Because we have $M_u = M_d$ the masses of each member of the various isospin multiplets are degenerate. Recall that the nucleon and Ξ masses were used to determine two of our NJL model parameters. All masses are in GeV.

	M_N	M_Λ	M_Σ	M_Ξ
NJL	0.940	1.120	1.234	1.318
Experiment	0.940	1.116	1.193	1.318

TABLE V. Numerical coefficients that define the Faddeev vertex functions for each member of the baryon octet. The nucleon, Σ, and Ξ vertex functions have the form given in Eq. (17) and the Λ vertex function is given in Eq. (18).

	α_1	α_2	α_3	α_4	α_5
Nucleon	0.418	0.013	−0.259	−0.018	0.366
Λ	0.364	0.278	−0.016	0.440	–
Σ	0.351	0.032	−0.215	−0.021	0.406
Ξ	0.388	0.017	−0.273	−0.015	0.364

where $q = p' - p$ is the 4-momentum transfer, $Q^2 \equiv -q^2$, and λ, λ' represent the initial and final baryon helicity, respectively. The scalar functions $G_A(Q^2)$, $G_P(Q^2)$, and $G_T(Q^2)$ label the axial, induced pseudoscalar, and induced pseudotensor form factors, respectively. In this work we restrict ourselves to the $q \to 0$ limit, where the current becomes

$$J^{\mu,a}_{5,\lambda}(p,p) = G_A(0)\,\bar{u}(p,\lambda)\,\gamma^\mu\gamma_5\,\lambda_a\,u(p,\lambda). \quad (27)$$

The flavor-triplet axial charge of an octet baryon g_A^B is given by the matrix element,

$$g_A^B\,s^\mu = \langle B|\bar{\psi}\,\gamma^\mu\gamma_5\,\lambda_3\,\psi|B\rangle = (\Delta u_B - \Delta d_B)\,s^\mu\,, \quad (28)$$

where $s^\mu = \bar{u}(p,\lambda)\,\gamma^\mu\gamma_5\,u(p,\lambda)$ is the spin vector of the octet baryon. The quark-spin fractions of the baryon are defined by

$$\Delta q_B\,s^\mu = \langle B|\bar{\psi}\,\gamma^\mu\gamma_5\,\hat{P}_q\,\psi|B\rangle, \quad (29)$$

where the u- and d-quark projection operators are given by

$$\hat{P}_q = \frac{1}{2}\left(\frac{2}{3}\,1 \pm \lambda_3 + \frac{1}{\sqrt{3}}\,\lambda_8\right), \quad (30)$$

and the plus sign corresponds to the u quark.

The various spin fractions for the octet baryons under consideration are given by the sum of the six Feynman diagrams represented in Fig. 4 and have the structure,

$$\Delta u_p = f^Q_{u[ud]} + f^Q_{u\{ud\}} + 2\,f^D_{u[ud]} + 2\,f^D_{u\{ud\}} + 4\,f^D_{d\{uu\}} + 2\,f^D_{u\{ud\}\leftrightarrow u[ud]}, \quad (31)$$

$$\Delta d_p = f^Q_{d\{uu\}} + 2\,f^D_{u[ud]} + 2\,f^D_{u\{ud\}} - 2\,f^D_{u\{ud\}\leftrightarrow u[ud]}, \quad (32)$$

$$\Delta u_{\Sigma^-} = 0, \quad (33)$$

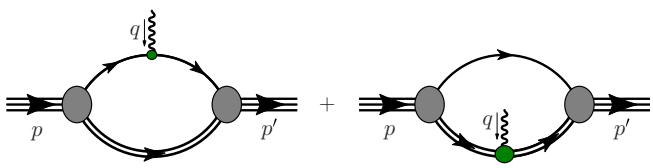

FIG. 4. (Color online) Feynman diagrams representing the axial current for the octet baryons. The diagram on the left is called the quark diagram and the one on the right the diquark diagram. In the diquark diagram the photon interacts with each quark inside the nonpointlike diquark.

$$\Delta d_{\Sigma^-} = f^Q_{d[ds]} + f^Q_{d\{ds\}} + 2\,f^D_{d[ds]} + 2f^D_{d\{ds\}} + 4\,f^D_{s\{dd\}} + 2\,f^D_{d\{ds\}\leftrightarrow d[ds]}, \quad (34)$$

$$\Delta u_{\Xi^-} = 0, \quad (35)$$

$$\Delta d_{\Xi^-} = f^Q_{d\{ss\}} + 2\,f^D_{s[ds]} + 2\,f^D_{s\{ds\}} - 2\,f^D_{s\{ds\}\leftrightarrow s[ds]}. \quad (36)$$

The nomenclature for these Feynman diagrams is as follows: A superscript Q implies that the operator acts directly on a quark (*quark diagram*) and a superscript D implies that the operator acts on (a quark inside) a diquark (*diquark diagram*); the notation $q_1[q_2q_3]$ indicates a diagram with quark content $q_1q_2q_3$ contains only a scalar diquark of quark content q_2q_3. Similarly the notation $q_1\{q_2q_3\}$ indicates a diagram contains only an axialvector diquark of quark content q_2q_3; and finally the notation $q_1\{q_2q_3\} \leftrightarrow q_1[q_2q_3]$ indicates the sum of the two diagrams where the operator induces a transition between scalar and axialvector diquarks of flavor q_2q_3. The numerical coefficients arise from the flavor structure of the operator and the Faddeev amplitude. Analogous expressions for the neutron, Σ^+, and Ξ^0 can easily be obtained using charge symmetry.

In general the quark diagram with a scalar diquark spectator reads

$$f^Q_{q_1[q_2q_3]}\,\overline{u}\,\gamma^\mu\gamma_5\,u = \overline{\Gamma}_{q_1[q_2q_3]}(p)\int\frac{d^4k}{(2\pi)^4} \times\; S_{q_1}(k)\,\gamma^\mu\gamma_5\,S_{q_1}(k)\,\tau_{[q_2q_3]}(p+k)\,\Gamma_{q_1[q_2q_3]}(p), \quad (37)$$

and the analogous diagram with an axialvector diquark spectator is given by

$$f^Q_{q_1\{q_2q_3\}}\,\overline{u}\,\gamma^\mu\gamma_5\,u = \overline{\Gamma}_{q_1\{q_2q_3\},\alpha}(p)\int\frac{d^4k}{(2\pi)^4} \times\; S_{q_1}(k)\,\gamma^\mu\gamma_5\,S_{q_1}(k)\,\tau^{\alpha\beta}_{\{q_2q_3\}}(p+k)\,\Gamma_{q_1\{q_2q_3\},\beta}(p). \quad (38)$$

Similarly, the general form of the diquark diagram with a scalar diquark reads

$$f^D_{q_1[q_2q_3]}\,\overline{u}\,\gamma^\mu\gamma_5\,u = \overline{\Gamma}_{q_1[q_2q_3]}(p)\int\frac{d^4k}{(2\pi)^4}\,i\,S_{q_1}(p+k) \times\; \tau_{[q_2q_3]}(k)\;\Lambda^\mu_{[q_2q_3]}\;\tau_{[q_2q_3]}(k)\,\Gamma_{q_1[q_2q_3]}(p), \quad (39)$$

and the analogous diagram with an axialvector diquark is given by

$$f^D_{q_1\{q_2q_3\}}\,\overline{u}\,\gamma^\mu\gamma_5\,u = \overline{\Gamma}_{q_1\{q_2q_3\},\alpha}(p)\int\frac{d^4k}{(2\pi)^4}\,i\,S_{q_1}(p+k) \times\; \tau^{\alpha\sigma}_{\{q_2q_3\}}(k)\;\Lambda^\mu_{\sigma\eta,\{q_2q_3\}}\;\tau^{\eta\beta}_{\{q_2q_3\}}(k)\,\Gamma_{q_1\{q_2q_3\},\nu}(p), \quad (40)$$

where $\Lambda^\mu_{[q_2q_3]}$ and $\Lambda^\mu_{\alpha\beta,\{q_2q_3\}}$ represent, respectively, the interaction of a scalar and axialvector diquark, with an axialvector current, in the $q \to 0$ and on-shell limits. Because the scalar diquark has spin zero, we have $\Lambda^\mu_{[q_2q_3]} = 0$, while for the

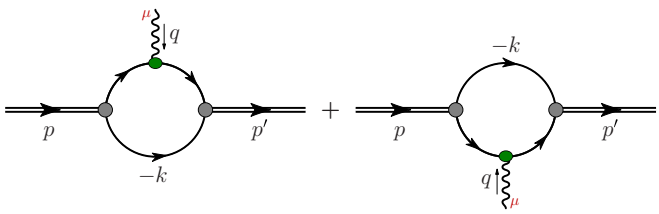

FIG. 5. (Color online) Feynman diagrams that represent the diquark axial current. The shaded circles are the diquark Bethe-Salpeter vertices and the shaded oval is the $\gamma^\mu\gamma_5$ vertex.

axialvector diquark we have

$$\Lambda^{\mu,\alpha\beta}_{\{q_2q_3\}}(p) = 3i\int\frac{d^4k}{(2\pi)^4} \times \mathrm{Tr}_D[\gamma^\beta\, S(p+k)\,\gamma^\mu\gamma_5\, S(p+k)\,\gamma^\alpha\, S(k)], \tag{41}$$

$$= g_A^{\{q_2q_3\}}\, i\varepsilon^{\mu\alpha\beta\lambda}p_\lambda, \tag{42}$$

where α is the inital and β the final diquark polarization. The Feynman diagram for this contribution is illustrated in Fig. 5. For the various axialvector diquarks we find $g_A^{\{\ell\ell\}} = -0.216$, $g_A^{\{\underline{\ell}s\}} = -0.194$, $g_A^{\{\ell\underline{s}\}} = -0.213$, and $g_A^{\{ss\}} = -0.194$.[7] Note that in evaluating Eq. (41) we have used the on-shell condition, $\varepsilon_\alpha(p)\,p^\alpha = 0$, for both the inital and final axialvector diquark.

The final Feynman diagram represents the mixing between the scalar and axialvector diquarks induced by the axial current; this diagram reads

$$f^D_{q_1[q_2q_3]\leftrightarrow q_1\{q_2q_3\}} \equiv f^D_{q_1[q_2q_3]\to q_1\{q_2q_3\}} + f^D_{q_1\{q_2q_3\}\to q_1[q_2q_3]}, \tag{43}$$

where each contribution is given by[8]

$$f^D_{q_1[q_2q_3]\to q_1\{q_2q_3\}}\,\bar{u}\,\gamma^\mu\gamma_5\,u = \overline{\Gamma}_{q_1\{q_2q_3\},\alpha}(p)\,i\int\frac{d^4k}{(2\pi)^4}, S_{q_1}(p+k)\,\tau^{\alpha\sigma}_{\{q_2q_3\}}(k) \times \Lambda^\mu_{\sigma,[q_2q_3]\to\{q_2q_3\}}\,\tau_{[q_2q_3]}(k)\,\Gamma_{q_1[q_2q_3]}(p), \tag{44}$$

$$f^D_{q_1\{q_2q_3\}\to q_1[q_2q_3]}\,\bar{u}\,\gamma^\mu\gamma_5\,u = \overline{\Gamma}_{q_1[q_2q_3]}(p)\,i\int\frac{d^4k}{(2\pi)^4},\, S_{q_1}(p+k)\,\tau_{[q_2q_3]}(k) \times \Lambda^\mu_{\sigma,\{q_2q_3\}\to[q_2q_3]}\,\tau^{\sigma\alpha}_{\{q_2q_3\}}(k)\,\Gamma_{q_1\{q_2q_3\},\alpha}(p). \tag{45}$$

[7] In our notation the underlined character denotes the quark that interacts with the photon. For example in $\{\underline{\ell}s\}$ the light quark interacts with the photon in the axialvector diquark.

[8] Note when calculating these diagrams we in practice consider a small momentum transfer so that we can correctly identify p'^2 and p^2 with the initial and final diquark mass squared.

TABLE VI. Results for the spin fractions in the proton, Σ^-, and Ξ^-. Analogous results for the neutron, Σ^+, and Ξ^0 can easily be obtained using charge symmetry.

Δu_p	Δd_p	Δu_{Σ^-}	Δd_{Σ^-}	Δu_{Ξ^-}	Δd_{Ξ^-}
1.145	0.331	0	−1.048	0	0.313

The diquark transition vertices are given by

$$\Lambda^{\mu\alpha}_{[q_2q_3]\to\{q_2q_3\}} = 3i\int\frac{d^4k}{(2\pi)^4} \times \mathrm{Tr}_D[\gamma_5\, S(p+k)\,\gamma^\mu\gamma_5\, S(p+k)\,\gamma^\alpha\, S(k)], \tag{46}$$

$$\Lambda^{\mu\alpha}_{\{q_2q_3\}\to[q_2q_3]} = 3i\int\frac{d^4k}{(2\pi)^4} \times \mathrm{Tr}_D[\gamma^\alpha\, S(p+k)\,\gamma^\mu\gamma_5\, S(p+k)\,\gamma_5\, S(k)]. \tag{47}$$

These vertices have the general form,

$$\Lambda^{\mu\alpha}_{[q_2q_3]\to\{q_2q_3\}} = a_{q_2q_3}\,g^{\mu\alpha} + b_{q_2q_3}\,p^\mu p^\alpha = -\Lambda^{\mu\alpha}_{\{q_2q_3\}\to[q_2q_3]}. \tag{48}$$

For the various diquark transitions we find $a_{\ell\ell} = -0.054$, $a_{\underline{\ell}s} = -0.052$, $a_{\ell\underline{s}} = -0.048$, $b_{\ell\ell} = 0.092$, $b_{\underline{\ell}s} = 0.096$, and $b_{\ell\underline{s}} = 0.115$.

Evaluating these diagrams gives the spin fractions which we summarize in Table VI. In addition to these body form factor contributions, the axial charge of the quark receives a finite renormalization. This renormalization is given by the inhomogeneous BSE illustrated in Fig. 6. The renormalized axial charge of the light quark is given by

$$g_A^q = \frac{1}{1 + 2\,G_{a_1}\,\Pi^{(T)}_{AA}(0)}, \tag{49}$$

where $\Pi^{(T)}_{AA}(q^2)$ is the transverse piece of the bubble diagram,

$$\Pi^{\mu\nu}_{AA}(q^2) = 6i\int\frac{d^4k}{(2\pi)^4}\mathrm{Tr}_D[\gamma^\mu\gamma_5\, S(k+q)\,\gamma^\nu\gamma_5\, S(k)], \equiv \left(g^{\mu\nu} - \frac{q^\mu q^\nu}{q^2}\right)\Pi^{(T)}_{AA}(q^2) + \frac{q^\mu q^\nu}{q^2}\,\Pi^{(L)}_{AA}(q^2). \tag{50}$$

The coupling G_{a_1} is adjusted ($G_{a_1} = 1.0$) to give $M_{a_1} = 1.26$ GeV. The unrenormalized quark axial charge is unity,

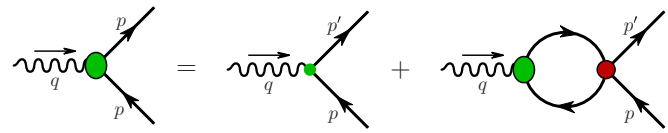

FIG. 6. (Color online) Inhomogeneous Bethe-Salpeter equation whose solution gives the quark-axialvector vertex, represented as the large shaded oval. The small dot is the inhomogeneous driving term ($\gamma^\mu\gamma_5$), while the shaded circle is the $\bar{q}q$ interaction kernel. Only the G_ρ interaction channel of Eq. (1) contributes.

TABLE VII. Axial charges for the beta decays with $\Delta S = 0$, corresponding to the three cases: Bare, treats the quark as a pointlike particle, without structure and without a meson cloud; BSE, includes the renormalization of the quark axial charge through the solution of the BSE and, finally, including the BSE renormalization as well as meson cloud corrections computed within the CBM. As the experimental result is only known for the nucleon case, for the Σ and Ξ we show the results from the CBM computation in Ref. [55], modified very slightly to reproduce the current experimental value of g_A^n.

	Bare	BSE	BSE + CBM	Expt. or Ref. [55]
$(g_A/f_1)^n$	1.48	1.38	1.27	1.2701 ± 0.0025
$(g_A/f_1)^\Sigma$	0.52	0.49	0.44	0.44
$(g_A/f_1)^\Xi$	−0.31	−0.29	−0.28	−0.32

however, for the renormalized axial charge we find $g_A^q = 0.935$. The value of the axial charge for octet baryon strangeness conserving transitions, for the bare case ("Bare") and for the case with a renormalized axial quark vertex ("BSE") are given in Table VII.

The axial charges for the octet baryons also receive corrections from the meson cloud. To preserve the correct nonanalytic behavior, required by chiral symmetry, it is easiest to compute these at the hadronic level [50,51]. This requires the meson-baryon coupling constants and form factors. The former are given by the appropriate Goldberger-Treiman relation, which is respected because the NJL model respects chiral symmetry. The latter are related to the hadron sizes. Because both the axial charges and hadron sizes in the present model are very close to those calculated in the cloudy bag model (CBM) [4,52], we can take the meson corrections directly from the work of Kubodera *et al.* [53]. In practice this means that our results should be multiplied by 0.92 for g_A^n, 0.90 for g_A^Σ, and 0.95 for g_A^Ξ. Our final results, including corrections from the quark vertex renormalization and the meson cloud are shown in Table VII. The only experimental value we have available is g_A^n. The values of the vector form factors $f_1(0)$ are 1, $\sqrt{2}$, and 1 for the nucleon, Σ, and Ξ, respectively. This comes from charge conservation when the electromagnetic form factors are computed in the octet.

We are now in a position to determine the size of SU(3)-flavor breaking effects for the axial charges of the octet baryons, using the SU(3)-flavor parametrization of Ref. [48], namely,

$$n \to p + \nu_e + e^- \Longrightarrow (g_A/f_1)^n = F + D, \quad (51)$$

$$\Sigma^- \to \Sigma^0 + \nu_e + e^- \Longrightarrow (g_A/f_1)^\Sigma = F, \quad (52)$$

$$\Xi^- \to \Xi^0 + \nu_e + e^- \Longrightarrow (g_A/f_1)^\Xi = F - D. \quad (53)$$

Within our model the values of F and D may be computed by choosing any pair of the previous relations. We call $F_{\Sigma(\Xi)}$ and $D_{\Sigma(\Xi)}$ the parameters calculated from $(g_A/f_1)^{\Sigma(\Xi)}$ and $(g_A/f_1)^n$. From Table VII we obtain

$$\begin{aligned} F_\Sigma &= (g_A/f_1)^\Sigma = 0.441, \\ D_\Sigma &= (g_A/f_1)^n - (g_A/f_1)^\Sigma = 0.829, \end{aligned} \quad (54)$$

and

$$\begin{aligned} F_\Xi &= \tfrac{1}{2}((g_A/f_1)^n + (g_A/f_1)^\Xi) = 0.496, \\ D_\Xi &= \tfrac{1}{2}((g_A/f_1)^n - (g_A/f_1)^\Xi) = 0.774. \end{aligned} \quad (55)$$

The discrepancies suggest SU(3)-flavor symmetry breaking effects of around 10%, with $F_\Sigma/F_\Xi = 0.89$ and $D_\Sigma/D_\Xi = 1.07$. Because the strangeness conserving β decays for the Σ^- and Ξ^- have not yet been measured, this result should be viewed as a prediction to be tested experimentally. We note that even larger SU(3) violation was reported in the context of the proton spin problem [54].

In addition, a comparison of our results with the cloudy bag model computations performed in Ref. [55] shows that g_A^Σ is the same in both models, whereas g_A^Ξ is slightly smaller in magnitude in our work. The calculation of Ref. [55] includes one-gluon exchange and center-of-mass corrections, plus recoil effects and a rescaling factor to reproduce the experimental g_A^n.

The other source of "data" with which our model might be compared are lattice QCD calculations. There has recently been good progress in the calculation of the electromagnetic form factors for the octet baryons [22,23], using chiral extrapolations of the lattice results. Clearly an extension of that work to weak form factors would provide a valuable test of our model predictions.

VI. CONCLUSIONS

We have computed the masses and the $\Delta S = 0$ axial charges of the baryon octet using a confining NJL model. The model results for the masses are in good agreement with the experimental values. While there are currently no measurements of the $\Delta S = 0$ axial charges, other than for the neutron, we did find very close agreement between our results and those found within the cloudy bag model. Because there is currently considerable discussion concerning the degree of violation of SU(3)-flavor symmetry, the deviation of order 10% which we found is significant.

It will be important to extend the present investigation to calculate the chiral corrections explicitly within this model. Given the new lattice results for octet baryon electromagnetic form factors, we look forward to simulations of a similar quality for the axial form factors. Meantime, it would be very interesting to extend the present model to calculate the hyperon electromagnetic form factors.

ACKNOWLEDGMENTS

I.C.C. thanks Wolfgang Bentz invaluable conversations. This material is based upon work supported by the U.S. Department of Energy, Office of Science, Office of Nuclear Physics, under Contract No. DE-AC02-06CH11357. We also acknowledge the Australian Research Council through the ARC Centre of Excellence in Particle Physics at the Terascale and an ARC Australian Laureate Fellowship FL0992247 (A.W.T.).

[1] A. Le Yaouanc, L. Oliver, O. Pene, and J.-C. Raynal, Phys. Rev. D **18**, 1591 (1978).
[2] N. Isgur and G. Karl, Phys. Rev. D **20**, 1191 (1979).
[3] A. Chodos, R. L. Jaffe, K. Johnson, and C. B. Thorn, Phys. Rev. D **10**, 2599 (1974).
[4] S. Theberge, A. W. Thomas, and G. A. Miller, Phys. Rev. D **22**, 2838 (1980); **23**, 2106 (1981).
[5] S. Theberge and A. W. Thomas, Phys. Rev. D **25**, 284 (1982).
[6] F. Myhrer, G. E. Brown, and Z. Xu, Nucl. Phys. A **362**, 317 (1981).
[7] F. Myhrer and Z. Xu, Phys. Lett. B **108**, 372 (1982).
[8] K. Tsushima, T. Yamaguchi, Y. Kohyama, and K. Kubodera, Nucl. Phys. A **489**, 557 (1988).
[9] H. Weigel, R. Alkofer, and H. Reinhardt, Nucl. Phys. A **576**, 477 (1994).
[10] G. Wagner, A. J. Buchmann, and A. Faessler, Phys. Rev. C **58**, 3666 (1998).
[11] D. Diakonov, in *Peniscola 1997, Advanced School on Non-Perturbative Quantum Field Physics* (World Scientific, Singapore, 1998), pp. 1–55.
[12] I. C. Cloët, D. B. Leinweber, and A. W. Thomas, Phys. Rev. C **65**, 062201 (2002).
[13] C. Boros and A. W. Thomas, Phys. Rev. D **60**, 074017 (1999).
[14] D. Diakonov, V. Petrov, P. Pobylitsa, M. V. Polyakov, and C. Weiss, Nucl. Phys. B **480**, 341 (1996).
[15] J. Beringer *et al.* (Particle Data Group), Phys. Rev. D **86**, 010001 (2012).
[16] S. Dürr, Z. Fodor, J. Frison, C. Hoelbling, R. Hoffmann, S. D. Katz, S. Krieg, T. Kurth *et al.*, Science **322**, 1224 (2008).
[17] R. D. Young and A. W. Thomas, Phys. Rev. D **81**, 014503 (2010).
[18] A. Walker-Loud, H.-W. Lin, D. G. Richards, R. G. Edwards, M. Engelhardt, G. T. Fleming, P. Hägler, B. Musch *et al.*, Phys. Rev. D **79**, 054502 (2009).
[19] S. Aoki *et al.* (PACS-CS Collaboration), Phys. Rev. D **79**, 034503 (2009).
[20] S. Borsanyi, S. Durr, Z. Fodor, C. Hoelbling, S. D. Katz, S. Krieg, L. Lellouch, T. Lippert *et al.*, arXiv:1406.4088.
[21] H.-W. Lin and K. Orginos, Phys. Rev. D **79**, 034507 (2009).
[22] P. E. Shanahan, R. Horsley, Y. Nakamura, D. Pleiter, P. E. L. Rakow, G. Schierholz, H. Stüben, A. W. Thomas, R. D. Young, and J. M. Zanotti (CSSM and QCDSF/UKQCD Collaborations), Phys. Rev. D **90**, 034502 (2014).
[23] P. E. Shanahan, A. W. Thomas, R. D. Young, J. M. Zanotti, R. Horsley, Y. Nakamura, D. Pleiter, P. E. L. Rakow *et al.*, Phys. Rev. D **89**, 074511 (2014).
[24] I. C. Cloët, R. Horsley, J. T. Londergan, Y. Nakamura, D. Pleiter, P. E. L. Rakow, G. Schierholz, H. Stüben *et al.*, Phys. Lett. B **714**, 97 (2012).
[25] J. Ashman *et al.* (European Muon Collaboration), Phys. Lett. B **206**, 364 (1988).
[26] F. Myhrer and A. W. Thomas, Phys. Lett. B **663**, 302 (2008).
[27] P. E. Shanahan, A. W. Thomas, K. Tsushima, R. D. Young, and F. Myhrer, Phys. Rev. Lett. **110**, 202001 (2013).
[28] I. C. Cloët, W. Bentz, and A. W. Thomas, Phys. Rev. C **90**, 045202 (2014).
[29] I. C. Cloët, C. D. Roberts, and A. W. Thomas, Phys. Rev. Lett. **111**, 101803 (2013).
[30] Y. Nambu and G. Jona-Lasinio, Phys. Rev. **122**, 345 (1961).
[31] Y. Nambu and G. Jona-Lasinio, Phys. Rev. **124**, 246 (1961).
[32] U. Vogl and W. Weise, Prog. Part. Nucl. Phys. **27**, 195 (1991).
[33] T. Hatsuda and T. Kunihiro, Phys. Rep. **247**, 221 (1994).
[34] S. P. Klevansky, Rev. Mod. Phys. **64**, 649 (1992).
[35] D. Ebert, T. Feldmann, and H. Reinhardt, Phys. Lett. B **388**, 154 (1996).
[36] G. Hellstern, R. Alkofer, and H. Reinhardt, Nucl. Phys. A **625**, 697 (1997).
[37] W. Bentz and A. W. Thomas, Nucl. Phys. A **696**, 138 (2001).
[38] N. Ishii, W. Bentz, and K. Yazaki, Nucl. Phys. A **587**, 617 (1995).
[39] N. Ishii, W. Bentz, and K. Yazaki, Phys. Lett. B **301**, 165 (1993).
[40] N. Ishii, W. Bentz, and K. Yazaki, Phys. Lett. B **318**, 26 (1993).
[41] I. R. Afnan and A. W. Thomas, Top. Curr. Phys. **2**, 1 (1977).
[42] A. Buck, R. Alkofer, and H. Reinhardt, Phys. Lett. B **286**, 29 (1992).
[43] I. C. Cloët, W. Bentz, and A. W. Thomas, Phys. Lett. B **621**, 246 (2005).
[44] I. C. Cloët, W. Bentz, and A. W. Thomas, Phys. Rev. Lett. **95**, 052302 (2005).
[45] I. C. Cloët, W. Bentz, and A. W. Thomas, Phys. Lett. B **659**, 214 (2008).
[46] W. Bentz, I. C. Cloët, T. Ito, A. W. Thomas, and K. Yazaki, Prog. Part. Nucl. Phys. **61**, 238 (2008).
[47] R. L. Jaffe and A. Manohar, Nucl. Phys. B **337**, 509 (1990).
[48] J. M. Gaillard and G. Sauvage, Ann. Rev. Nucl. Part. Sci. **34**, 351 (1984).
[49] H. Hogaasen and F. Myhrer, Z. Phys. C **68**, 625 (1995).
[50] A. W. Thomas and G. Krein, Phys. Lett. B **456**, 5 (1999).
[51] A. W. Thomas and G. Krein, Phys. Lett. B **481**, 21 (2000).
[52] A. W. Thomas, Adv. Nucl. Phys. **13**, 1 (1984).
[53] K. Kubodera, Y. Kohyama, K. Oikawa, and C. W. Kim, Nucl. Phys. A **439**, 695 (1985).
[54] S. D. Bass and A. W. Thomas, Phys. Lett. B **684**, 216 (2010).
[55] T. Yamaguchi, K. Tsushima, Y. Kohyama, and K. Kubodera, Nucl. Phys. A **500**, 429 (1989).